PATHOPHYSIOLOGICAL MECHANISMS OF MUCOCILIARY CLEARANCE FUNCTION IN PATIENTS WITH RESPIRATORY AND OLFACTORY DISORDERS OF FUNCTIONAL-MECHANICAL AND VIRAL ORIGIN

Bondarenko Ya.D.[1, 2], Shushliapina N.O.[1], Kalashnyk-Vakulenko Yu.M.[1], Yashchenko M.I.[1]

[1]Kharkiv National Medical University, Kharkiv, Ukraine
[2]Friedrich-Alexander University of Erlangen–Nuremberg (FAU), Erlangen, Germany

https://doi.org/10.35339/ic.2025.12.4.bsk

ABSTRACT

Background. MucoCiliary Clearance (MCC) is the primary protective mechanism of the upper respiratory tract. Differentiating between extracellular (functional-mechanical) and intracellular (viral cytopathic) mechanisms of MCC impairment has been studied insufficiently but critical for selecting adequate therapeutic strategies.

Aim. To investigate the pathophysiological mechanisms of MCC in patients with respiratory and olfactory disorders depending on the duration and degree of nasal obstruction, and in patients post-Coronavirus Disease 2019.

Materials and Methods. A prospective observational study included 196 patients (mean age [37.4±13.1] years) with nasal obstruction and impaired respiratory/olfactory functions (disease duration from 1 month to 5 years). Patients were divided into four groups: Group 1 (n=53) – pronounced chronic nasal obstruction ([3–5] years); Group 2 (n=48) – partial obstruction (up to 6 months); Group 3 (n=44) – pronounced obstruction (up to 1 month); Group 4 (n=51) – acute post-viral rhinosinusitis after Severe Acute Respiratory Syndrome Coronavirus 2. Two pathogenetic profiles were evaluated: functional-mechanical (groups 1–3) and viral cytopathic (Group 4). Assessment included rhinomanometry, Saccharin Transit Time (STT), olfactometry (Sniffin' Sticks), and high-speed video microscopy of ciliary epithelium (×100, 120 frames/s) analyzed in ImageJ/ciliaFA. Statistical processing of the data was performed using one-way analysis of variance (ANOVA) with post hoc Student's test and Bonferroni correction and Pearson correlation with Excel 2022 (Microsoft, USA). The article is a part of scientific research with state registration number 0125U001264.

Research Ethics. The study complied with the World Medical Association Declaration of Helsinki (1964–2024) and relevant Ministry of Health of Ukraine orders. All participants provided written informed consent.

Results. In Group 1, aerodynamic resistance was [3.1±0.4] kPa·s/L, STT was [24.5±3.1] min, and ciliary beat frequency (CBF) was [7.3±1.4] Hz; metachronal wave was absent in 100% of cases, with hyposmia in 100% ([4.1±1.3] points). In Group 2, STT was [18.0±2.4] min, CBF was [7.6±3.1] Hz; in Group 3, STT was [34.7±3.3] min, CBF was [6.8±2.2] Hz. In Group 4, resistance was [1.9±0.4] kPa·s/L, STT was [17.0±1.9] min, and CBF was [8.1±1.4] Hz. Here, anosmia was present in 31.6% ([0.9±0.5] points) and hyposmia in 68.4% ([4.1±0.9] points).

Conclusions. Two fundamentally different pathophysiological profiles of MCC dysfunction were identified: functional-mechanical origin (groups 1–3) and viral cytopathic origin (Group 4), requiring diametrically opposite therapeutic strategies.

Keywords: *otorhinolaryngology, ciliary epithelium, nasal obstruction, olfactory dysfunction, COVID-19, rhinomanometry.*

Corresponding Author:

Bondarenko Ya.D. – Student of the Kharkiv National Medical University, Ukraine; Student of the Friedrich-Alexander University of Erlangen–Nuremberg (FAU), Germany.

✉ 4, Nauky ave., Kharkiv, Ukraine, 61022.

E-mail: bondarenkoyaroslav2017@gmail.com

Introduction

MucoCiliary Clearance (MCC) is the main protective mechanism of the upper respiratory tract, ensuring continuous transport of mucus from the nasal cavity to the nasopharynx due to the coordinated beating of the ciliary epithelium [1; 2]. Ciliary Beat Frequency (CBF) and the saccharin Transit Time Test (STT) are sensitive functional

indicators of the condition of the nasal mucosa [3]. Current data indicate that the relationship between the degree of nasal obstruction and impairment of MCC is complex and depends not only on mechanical narrowing of the nasal passages but also on the severity of inflammation, epithelial remodeling, and the nature of the pathological process [4; 5]. Postviral dysfunction of MCC occurs as a result of direct cytopathic damage to the ciliary epithelium and has a distinct pathophysiological mechanism that requires a different therapeutic approach [6]. In this regard, clinical phenotyping of MCC dysfunction is fundamentally important, since functional-mechanical and viral cytopathic forms require different treatment strategies [7; 8]. Architectural anomalies of the nasal cavity – deviation of the nasal septum, concha bullosa, hypertrophy of the inferior nasal turbinates – create mechanical obstacles to physiological airflow, disrupt the transport of odorants to the olfactory cleft, and cause pathological turbulence in the nasal cavity [9–11]. In contrast, in postviral sensorineural dysfunction, damage to the olfactory epithelium is predominantly cellular in nature; therefore, only surgical or standard anti-inflammatory treatment does not provide significant functional recovery [12; 13].

The research hypothesis is that impairment of mucociliary clearance in nasal obstruction may be formed by different pathophysiological mechanisms – functional-mechanical and viral cytopathic – which differ in functional indicators and clinical course. The practical value of this approach lies in the possibility of using accessible functional methods for differential diagnosis and selection of further pathogenetically substantiated therapy.

The **aim** of the study was to investigate the pathophysiological mechanisms of mucociliary clearance function in patients with respiratory and olfactory disorders of functional and viral origin depending on the duration and degree of nasal obstruction, as well as in patients who have had COronaVIrus Disease 2019 (COVID-19).

Materials and Methods

The prospective observational study included 196 patients (mean age [37.4±13.1] years) with varying degrees of nasal obstruction combined with impairment of respiratory and olfactory function (disease duration from 1 month to 5 years), divided into four groups according to the clinical picture and duration of the disease. Group 1 consisted of 53 patients (27.0%) with pronounced impairment of nasal breathing lasting for [3–5] years, Group 2 – 48 patients (24.5%) with partial nasal obstruction lasting up to 6 months, Group 3 – 44 patients (22.5%) with pronounced impairment of nasal breathing lasting up to 1 month, Group 4 – 51 patients (26.0%) with acute postviral rhinosinusitis associated with SARS-CoV-2 (Severe Acute Respiratory Syndrome Coronavirus 2), lasting up to 3 months. The study included individuals in the absence of local or systemic antibiotic therapy during the previous 6 weeks, chronic systemic diseases, a burdened family history of hereditary diseases, as well as concomitant pharmacotherapy capable of modifying MCC. Patients with chronic rhinosinusitis with or without polyps, systemic immunodeficiency, autoimmune pathologies, and pharmacological interventions capable of modulating MCC were excluded.

Clinical examination included ENT (Ear, Nose and Throat) examination with endoscopy of the nasal cavity, rhinomanometry (computer rhinomanometer TNDA-PVH, forced mode, calculation of aerodynamic resistance coefficient) and olfactometry using the Sniffin' Sticks system (Burghardt®, Germany) [14]. The latter included a threshold test with 16 triplets of n-butanol markers with descending concentration (anosmia – 1 point, hyposmia – [2–6] points, normosmia – [7–16] points) and an identification test with 12 household odors (anosmia – [0–6] points, hyposmia – [7–10] points, normosmia – [11–12] points). Assessment of MCC was performed using the saccharin transit time test [15], where values of [7–15] min were considered normal and more than 20 min – pathological [16], as well as by determining Ciliary Beat Frequency (CBF). The material was obtained by brush scraping, placed in phosphate buffer (37°C) and examined at ×100 magnification on a Karl Zeiss PrimoStar microscope with a Sigeta TCMOS5100 video camera. Video recording was performed at a speed of 120 frames/s for 1 minute; CBF was calculated using the formula:

$$CBF = N \times fps / K \quad (1),$$

where N – 10 cycles, fps – 120 frames/s, K – the number of frames per 10 cycles [3].

The normality of data distribution was assessed using the Shapiro-Wilk test. Since data was distributed normally, parametric statistical methods were chosen for further analysis. Statistical processing of the data was performed using one-way analysis of variance (ANOVA) with post hoc Student's test and Bonferroni correction, and Pearson

correlation analysis was used to assess the relationships between disease duration and functional parameters. The data are presented as M±SD; calculations were performed in Excel 2022 (Microsoft, USA).

Research Ethics

The study was conducted in accordance with the ethical standards of the World Medical Association Declaration of Helsinki (1964–2024), Directive 86/609 of the European Community, and Order No.690 of the Ministry of Health of Ukraine dated September 23, 2009. Written informed consent was obtained from all participants.

Results

From the total cohort of 196 patients, two pathophysiological profiles of MCC dysfunction were identified. For the assessment of functional-mechanical origin Groups 1 (n=53; 27.0%), 2 (n=48; 24.5%), and 3 (n=44; 22.5%) were selected – a total of 145 patients (74.0%) with varying degrees and duration of structurally determined nasal obstruction. Viral cytopathic origin was represented by Group 4 (n=51; 26.0%) – patients with postviral rhinosinusitis after SARS-CoV-2.

"Aerodynamic resistance syndrome" – functional-mechanical origin (groups according to the degree and duration of obstruction) (n=145; 74.0%). Group 1 consisted of 53 patients (27.0%) with structural ENT pathology (deviation of the nasal septum, hypertrophy of the inferior nasal turbinates and/or concha bullosa) and disease duration of [3–5] years (persistent pathology). The patients complained of unilateral or bilateral nasal congestion, a feeling of pressure in the paranasal sinuses, impaired nasal breathing during exertion, and inability to blow the nose due to thick secretion. Endoscopic examination revealed a hyperemic, edematous, and pasty mucosa with strands of viscous mucus.

Rhinomanometry revealed consistently high aerodynamic resistance [3.1±0.4] kPa·s/L (pronounced nasal obstruction), which significantly exceeds the values of Group 2 ([2.2±0.5] kPa·s/L). The mean STT was [24.5±3.1] min – twice the upper limit of normal ([7–15] min).

Olfactometry revealed hyposmia in 100% of patients in Group 1 according to the threshold test – [4.1±1.3] points. The identification test showed hyposmia in 48.3% ([10.3±1.4] points) and normosmia in 51.7% ([11.8±1.7] points). The olfactory disorder was characterized as conductive hyposmia: a mechanical obstacle to the access of odorants to the olfactory cleft due to edema and obstruction, rather than primary neuroepithelial damage.

High-speed video microscopy (×100, 120 frames/s) confirmed that the cilia were morphologically preserved but functionally blocked by an external physical factor, as shown in *Figure 1*. CBF was moderately reduced – mean [7.3±1.4] Hz (physiological norm ~[12–15] Hz). The beating pattern demonstrated pronounced disturbances: the effective stroke was shortened or absent, the movement acquired a pendulum-like, rigid character with significantly reduced amplitude and loss of synchrony. The metachronal wave was absent in 97% of cases.

The pathological process is extracellular, which is confirmed by a direct relationship between aerodynamic resistance [3.1±0.4] kPa·s/L, disease duration ([3–5] years), and suppression of MCC (STT [24.5±3.1] min, CBF [7.3±1.4] Hz). Anatomical obstacles disrupt the physiological laminar nasal airflow, generating turbulence with

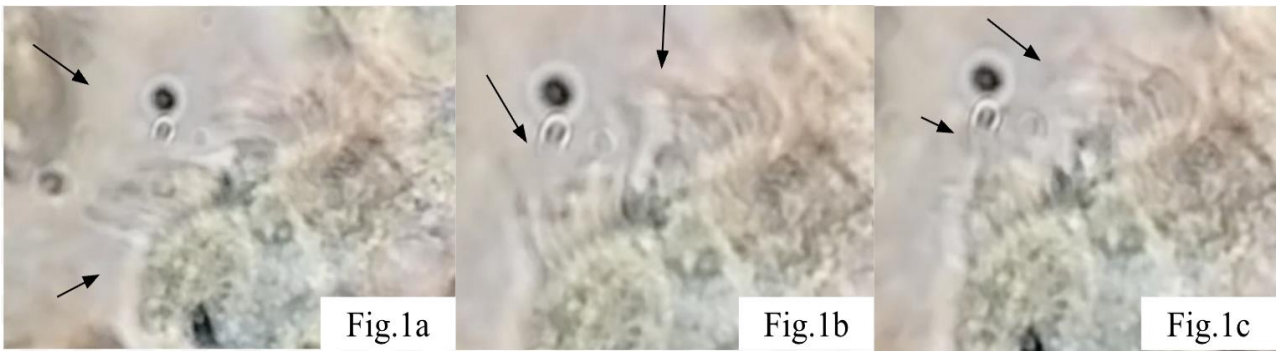

Fig. 1. High-speed video microscopy, freeze frame: a) beginning of the cycle: ciliary hypokinesia, minimal amplitude; b) middle of the cycle: irregular pattern, pronounced asynchrony of beating; c) completion: weakened metachronal wave, unstable trajectory. Magnification × 1000, the preparation is not colored

vortex zones and locally increased pressure on certain areas of the epithelium [17; 18]. Turbulent airflow, in turn, evaporates the periciliary fluid, the surface mucus layer thickens and physically deposits on the cilia, mechanically limiting their movement (zol-gel layer imbalance, or the "drying effect"), which partially coincides with the results of Bustamante-Marin X.M. et al. (2017) [19] and Button B. et al. (2012) [20]. At the same time, increased mechanical shear stress activates mechanosensitive ion channels TRPV4, triggering a calcium-dependent cascade [21], which stimulates goblet cells to massive hypersecretion of mucin MUC5AC [22] with a sharp increase in secretion viscosity [23]. One of the theories of energy generation is the continuation of generation by the dynein ATPase arm and the difficulty in overcoming the resistance of hyperconcentrated MUC5AC mucus [19; 20] [21; 22]. Observation of the clinical status of mucosal hydration in patients of Groups 1, 2, 3 corresponds to the above-mentioned mechanism. A schematic representation of the pathogenesis is shown in *Figure 2*.

Comparative analysis of functional-mechanical origin revealed the nature of MCC dysfunction depending on the degree and duration of obstruction. The most pronounced suppression of MCC was observed in acute obstruction (Group 3), even with short duration (STT [34.7±3.3] min, CBF [6.8±2.2] Hz). At the same time, in subacute moderate obstruction (Group 2), predominantly reversible, conductive olfactory function disorders were noted (STT [18.0±2.4] min, CBF [7.6±3.1] Hz).

"Postviral cytopathic origin" – Group 4 (n=51; 26.0%). The mechanism of MCC impairment is fundamentally different: direct destruction of cellular structural elements at the molecular level, rather than external aerodynamic factors [3; 12; 24].

The main complaint was persistent loss or distortion of smell: anosmia in 27.5% of patients, dysosmia/parosmia in most of the remaining patients with minimal impairment of nasal breathing. Endoscopic examination revealed intact nasal architecture; the mucosa appeared pale, with mode-

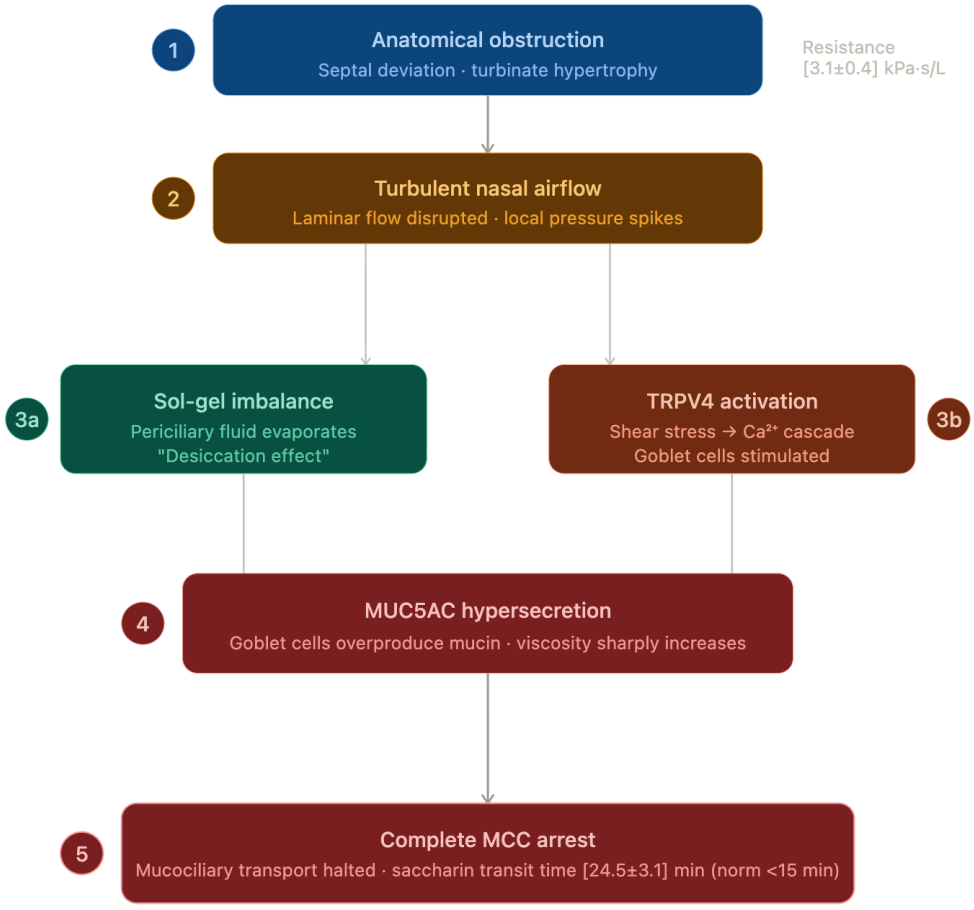

Fig. 2. Pathophysiological mechanism of aerodynamic syndrome

rate signs of active inflammation or edema – an endoscopic profile diametrically opposite to Group 1, which was confirmed by rhinomanometric data in the form of aerodynamic resistance [1.9±0.4] kPa·s/L, which was within the physiological range. This sharply contrasts with the subjective sensation of lack of air in patients of observation Groups 1 and 3. The mean STT was [17.0±1.9] min (range [16–23] min). It is fundamentally important that the use of decongestants had no effect on STT – a key differential marker confirming organic, structural damage [3].

Olfactometry confirmed deep sensorineural dysfunction. Threshold test: anosmia in 31.6% – [0.9±0.5] points; hyposmia in 68.4% – [4.1±0.9] points in the threshold test and [8.2±1.3] points in the identification test. The pathogenetic substrate is direct damage to the supporting cells of the olfactory epithelium via ACE2/TMPRSS2 receptors, which determines the sensorineural nature of the olfactory disorder [25].

Video microscopy revealed kinematic disturbances. CBF was within normal limits in 59% and moderately reduced in 41% (range [7–9] Hz), mean [8.1±1.4] Hz. Despite the relatively preserved frequency, the beating pattern demonstrated profound qualitative disturbances: shortened effective stroke, vibratory movement, asynchrony between adjacent cells, reduced amplitude. Metachronal activity was irregular and fragmented. The obtained data are shown in *Figure 3*.

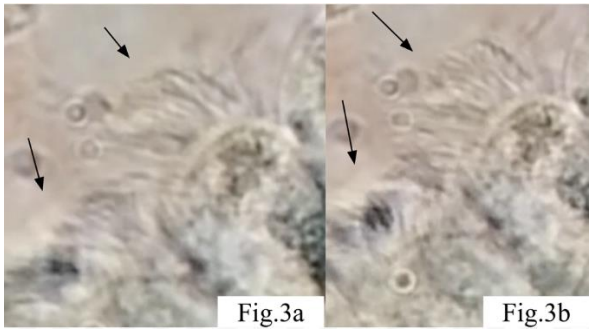

Fig. 3. Video microscopy of ciliary epithelium, freeze frame: a) effective stroke phase (movement vector indicated by an arrow); b) recovery stroke phase; dyskinesia: vibratory movement and shortened amplitude. Magnification × 1000, the preparation is not stained.

The pathophysiological mechanism of SARS-CoV-2 begins with viral entry into cells via ACE2 and TMPRSS2 receptors, abundantly expressed on supporting cells of the olfactory epithelium and ciliated cells of the respiratory tract, initiating direct cytotoxicity and an intracellular inflammatory response [25]. Viral replication is accompanied by pronounced mitochondrial damage and decreased ATP synthesis, which limits the energy supply of dynein ATPase motors and gradually reduces the force, amplitude, and coordination of ciliary beating [26; 27]. In parallel, cytoskeletal remodeling occurs: the virus disrupts the structure of microtubules, leading to impaired ciliary movement [27–29]. Dysfunction of Celsr1 signaling disorganizes basal bodies, reducing mucociliary transport [29–32]. At the final stage, cells lose the ciliary apparatus (deciliation), completely stopping clearance. Restoration of cilia requires 3–6 months [33]. The proposed mechanism is shown in *Figure 4*. The main clinical and functional differences between the groups are presented in *Table 1*.

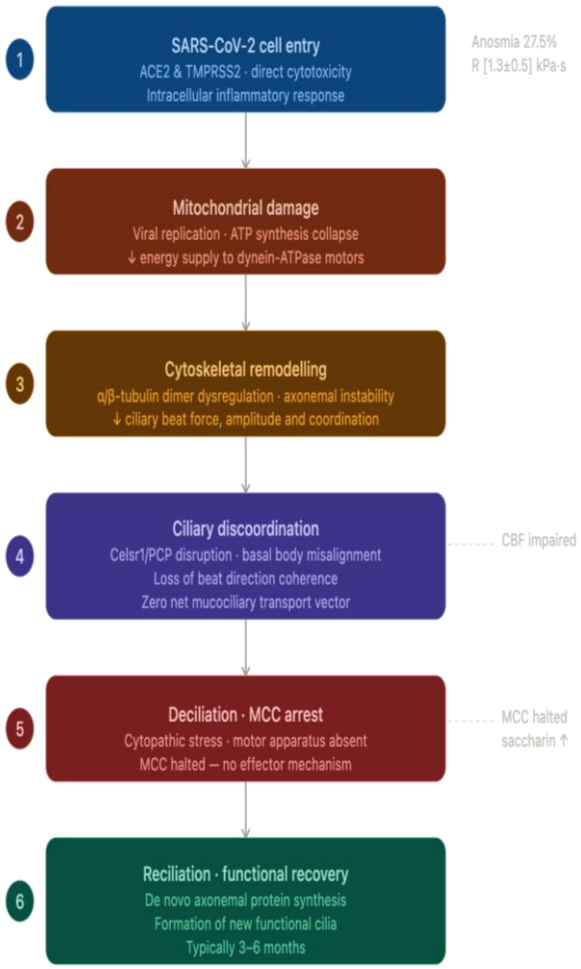

Fig. 4. Intracellular pathophysiology of Group 4 post-COVID mucociliary dysfunction: from SARS-CoV-2 cell entry to deciliation and recovery.

Table 1. Main clinical and functional parameters in patients with functional-mechanical (Groups 1, 2, 3) and viral (Group 4) origin of MCC dysfunction (M±SD)

Parameter	Group 1 (n=53) Functional max., [3–5] years	Group 2 (n=48) Functional max., 6 months	Group 3 (n=44) Functional max., ≤1 months	Group 4 (n=51) COVID-19, ≤3 months
Disease duration	[3–5] years (chronic)	Up to 6 months	Up to 1 month	Up to 3 months
Rhinomanometry (kPa·s/L)	3.1±0.4	2.2±0.5	3.6±0.4	1.9±0.4
STT (min)	24.5±3.1	18.0±2.4	34.7±3.3	17.0±1.9
CBF (Hz)	7.3±1.4	7.6±3.1	6.8±2.2	8.1±1.4
Olfactory threshold test (scores)	Hyposmia (4.1±1.3)	Mild hyposmia (5.6±2.2)	Hyposmia (3.4±2.4)	Anosmia 31.6% (0.9±0.5) / Hyposmia 68.4% (4.1±0.9)
Identification test (scores)	Hyposmia – 48.3% (10.3±1.4) / Normosmia – 51.7% (11.8±1.7)	Normosmia – 81.3%	Moderate hyposmia – 62.7% (9.3±1.4)	Anosmia (0.9±0.5) / Hyposmia (4.1±0.9)
Metachronal wave	Absent – 100%	Partially preserved	Reduced coordination	Fragmented, irregular
Ciliary beating pattern	Pendulum-like, reduced amplitude, no effective stroke	Mostly normal, mild changes	Disorientation, irregular cycle	Dyskinesia: vibration, asynchrony, reduced amplitude
Effect of decongestants on STT	Transient improvement	Moderate improvement	Marked improvement	Absent

Notes: M±SD – mean ± standard deviation;
MCC – mucociliary clearance;
CBF – ciliary beat frequency;
STT – saccharin transit time.
Statistical analysis: ANOVA with post hoc Student's t-test and Bonferroni correction; Pearson correlation (Excel 2022, Microsoft, USA).

Discussion

The study confirmed a pronounced impact of nasal obstruction on ciliary epithelial function and identified two fundamentally different pathophysiological profiles of MCC dysfunction. Similar conclusions were reported by Jang Y.J. et al. (2002), who described histological changes of the nasal mucosa in severe obstruction caused by septal deviation. These included a significantly lower ciliary density score on the concave side ([1.8±±0.69] vs [2.8±0.95]; p=0.005), markedly higher inflammatory cell infiltration ([102.5±51.8] vs [52.9±4.95]; p=0.003), and a reduced number of glandular acini ([66.6±18.7] vs [97.2±16.9]; p<0.001), further supporting these findings [34]. From an aerodynamic perspective, these data are consistent with previous studies [35; 36].

In Group 1, a direct correlation between aerodynamic resistance ([3.1±0.4] kPa·s/L), disease duration ([3–5] years), and MCC suppression (STTT [24.5±3.1] min, CBF [7.3±1.4] Hz) confirms a functional-mechanical origin. The duration-dependent nature of MCC dysfunction is supported by comparison with Group 2 (STTT [18.0±2.4] min, CBF

[7.6±3.1] Hz) and Group 3 (STTT [34.7±3.3] min, CBF [6.8±2.2] Hz). The pathophysiological mechanism is based on studies explaining the TRPV4–MUC5AC signaling cascade, involving activation of mechanosensitive ion channels under shear stress from turbulent airflow, followed by hypersecretion of MUC5AC by goblet cells. This represents a molecular mechanism for the formation of pathologically viscous mucus, which physically obstructs morphologically intact cilia [21; 22].

In Group 4, the combination of moderate aerodynamic resistance ([1.9±0.4] kPa·s/L) with pronounced olfactory dysfunction (anosmia 31.6%) and a pathological ciliary beating pattern, despite relatively preserved CBF ([8.2±1.3] Hz), indicates a viral cytopathic effect. Damage to ACE2/TMPRSS2 and loss of Celsr1 polarity result in impaired MCC despite preserved beating intensity [28–34]. Similar findings were reported by Schreiner T. et al. (2022), who demonstrated that acute COVID-19 leads to a progressive decline in FOXJ1+ cells (median 30.24% in controls vs 4.44% on day 14; p=0.020), along with ciliary loss (median 1.85% on day 3 vs 39.29% in controls; p<0.001) and the emergence of axonemal ultrastructural abnormalities such as compound cilia even after ciliogenesis recovery (median 2% vs 0% in controls; p=0.041), indicating dysregulated epithelial regeneration [29]. Oliveira B.R. et al. (2024), in turn, demonstrated that interaction of the SARS-CoV-2 spike protein (WT, Alpha, Delta variants) with SH-SY5Y neuronal cells disrupts the β-tubulin network and increases cathepsin L secretion independently of productive infection, suggesting an extracellular mechanism of cytoskeletal alterations [27].

Conclusions

1. Two fundamentally different pathophysiological profiles of mucociliary clearance (MCC) dysfunction were identified: Groups 1–3 – functional-mechanical origin, and Group 4 – viral cytopathic origin. This differentiation enables the development of pathogenetically grounded therapeutic strategies.

2. In Group 1, a direct correlation between aerodynamic resistance ([3.1±0.4] kPa·s/L), disease duration ([3–5] years), and MCC suppression (STTT [24.5±3.1] min, CBF [7.3±1.4] Hz) confirms the functional-mechanical origin of the disease and is associated with an increased risk of irreversible impairment. However, in the context of surgical planning, functional recovery may be achieved through operative intervention, as supported by previous studies. Groups 2 and 3 demonstrate a similar mechanism; however, due to shorter disease duration, these patients have a more favorable prognosis and greater potential for recovery.

3. In Group 4, moderate aerodynamic resistance ([1.9±0.4] kPa·s/L), combined with pronounced sensorineural olfactory dysfunction (anosmia 31.6%) and pathological ciliary kinematics, confirms a viral cytopathic profile of injury. This profile requires not only pathogenetically oriented anti-inflammatory therapy but also consideration of further neurorehabilitation of the olfactory system.

Funding and Acknowledgments

The research was conducted as a private initiative of the authors, did not receive funding from grant programs, and the research topic was not officially registered in the state register of scientific topics.

Declarations

Conflict of interest is absent.

All authors have given their consent to the publication of the article under the terms of the Creative Commons Attribution-NonCommercial-ShareAlike 4.0 International License and a public agreement with the publisher, to the processing and publication of their personal data.

The authors state that in the process of conducting research, preparing, and editing this manuscript, they did not use any generative AI tools or services to perform any of the tasks listed in the Generative AI Delegation Taxonomy (GAIDeT, 2025). All stages of work (from the development of the research concept to the final editing) were carried out without the involvement of generative artificial intelligence, exclusively by the authors.

Authors' Contributions

Contribution / Authors	A	B	C	D	E	F
Bondarenko. Ya.D.	+	+	+	+	+	+
Shushliapina N.O.	+		+	+		+
Kalashnyk-Vakulenko Yu.M.	+	+	+		+	+
Yashchenko M.I.					+	+

Notes: A – concept; B – design; C – data collection; D – statistical processing and interpretation of data; E – writing or critical editing of the article; F – approval of the final version for publication and agreement to be responsible for all aspects of the work.

References

1. Comba A, Atan D. Evaluation of nasal mucociliary clearance time in children with celiac disease. Int J Pediatr Otorhinolaryngol. 2020;133:109936. DOI: 10.1016/j.ijporl.2020.109936. PMID: 32088546.

2. Cohen NA. Sinonasal mucociliary clearance in health and disease. Ann Otol Rhinol Laryngol Suppl. 2006;196:20-6. DOI: 10.1177/00034894061150s904. PMID: 17040014.

3. Svitlychna YV, Shushliapina NO, Lupyr AV, Bondarenko YD. Analysis of the relationship between nasal mucosa mucociliary clearance parameters and the duration and severity of nasal obstruction. Medicine Today and Tomorrow. 2025;94(3):10p. DOI: 10.35339/msz.2025.94.3.ssl.

4. Kumar L, Belaldavar BP, Bannur H. Influence of deviated nasal septum on nasal epithelium: an analysis. Head Neck Pathol. 2017;11(4):501-5. DOI: 10.1007/s12105-017-0819-9. PMID: 28474294.

5. Babchenko NV. The condition of mucociliary clearance in patients with nasal septum deviation and postnasal drip syndrome. Clin Prev Med. 2023;9(26):53-6. DOI: 10.31612/2616-4868.4(26).2023.08.

6. Hu B, Gong M, Xiang Y, Qu S, Zhu H, Ye D. Mechanism and treatment of olfactory dysfunction caused by coronavirus disease 2019. J Transl Med. 2023;21(1):829. DOI: 10.1186/s12967-023-04719-x. PMID: 37978386.

7. Bondarenko Y, Kochnieva O, Kotsar O, Kauk O, Pionova O, Tsyhanenko O, et al. CRISPR-edited commensals of the nasopharynx as platform for developing next-generation microbial probiotics. Proceeding of the Shevchenko Scientific Society. Medical Sciences. 2025;77(2). doi: 10.25040/ntsh2025.02.16.

8. Avrunin OG, Tymkovych MYu, Abdelhamid IY, Shushliapina NO, Nosova YV, Semenets VV. Features of image segmentation of the upper respiratory tract for planning of rhinosurgical surgery. Proc ELNANO. 2019:485-8. doi: 10.1109/ELNANO.2019.8783739.

9. Doty RL, Mishra A. Olfaction and its alteration by nasal obstruction, rhinitis, and rhinosinusitis. Laryngoscope. 2001;111(3):409-23. DOI: 10.1097/00005537-200103000-00008. PMID: 11224769.

10. Zhao K, Scherer PW, Hajiloo SA, Dalton P. Effect of anatomy on human nasal air flow and odorant transport patterns: implications for olfaction. Chem Senses. 2004;29(5):365-79. DOI: 10.1093/chemse/bjh033. PMID: 15201204.

11. Li C, Jiang J, Kim K, Otto BA, Farag AA, Cowart BJ, et al. Nasal structural and aerodynamic features that may benefit normal olfactory sensitivity. Chem Senses. 2018;43(4):229-37. DOI: 10.1093/chemse/bjy013. PMID: 29555355.

12. Shushliapina N, Kalashnyk-Vakulenko Y, Bondarenko Y. Symptomatic treatment of dysosmia in rhinological pathology of functional and viral (SARS-CoV-2) origin. Inter Collegas. 2025;12(3):7p. DOI: 10.35339/ic.2025.12.3.skb.

13. Grabosky A, Mackers P, Langdon C, Alobid I. Change in olfactory function after septoplasty. A systematic review and meta-analysis. Rhinology. 2021;59(2):144-50. DOI: 10.4193/Rhin20.252. PMID: 33320116.

14. Rumeau C, Nguyen DT, Jankowski R. How to assess olfactory performance with the Sniffin' Sticks test®. Eur Ann Otorhinolaryngol Head Neck Dis. 2016;133(3):203-6. DOI: 10.1016/j.anorl.2015.08.004. PMID: 26344139.

15. Rutland J, Cole PJ. Nasal mucociliary clearance and ciliary beat frequency in cystic fibrosis compared with sinusitis and bronchiectasis. Thorax. 1981;36(9):654-8. DOI: 10.1136/thx.36.9.654. PMID: 7314040.

16. Deborah S, Prathibha KM. Measurement of nasal mucociliary clearance. Clin Res Pulmonol. 2014;2(2):14-9. DOI: 10.47739/2333-6625/1019.

17. Churchill SE, Shackelford LL, Georgi JN, Black MT. Morphological variation and airflow dynamics in the human nose. Am J Hum Biol. 2004;16(6):625-38. DOI: 10.1002/ajhb.20074. PMID: 15495232.

18. Wang DY, Lee HP, Gordon BR. Impacts of fluid dynamics simulation in study of nasal airflow physiology and pathophysiology in realistic human three-dimensional nose models. Clin Exp Otorhinolaryngol. 2012;5(4):181-7. DOI: 10.3342/ceo.2012.5.4.181. PMID: 23275797.

19. Bustamante-Marin XM, Ostrowski LE. Cilia and mucociliary clearance. Cold Spring Harb Perspect Biol. 2017;9(4):a028241. DOI: 10.1101/cshperspect.a028241. PMID: 27815315.

20. Button B, Cai LH, Ehre C, Kesimer M, Hill DB, Sheehan JK, et al. A periciliary brush promotes the lung health by separating the mucus layer from airway epithelia. Science. 2012;337(6097):937-41. DOI: 10.1126/science.1223012. PMID: 22923584.

21. Ueda T, Hoshikawa M, Shibata Y, Kumamoto N, Ugawa S. Basal cells express functional TRPV4 channels in the mouse nasal epithelium. Biochem Biophys Rep. 2015;4:169-74. DOI: 10.1016/j.bbrep.2015.09.008. PMID: 29124151.

22. Kim YJ, Cho HJ, Shin WC, Song HA, Yoon JH, Kim CH. Hypoxia-mediated mechanism of MUC5AC production in human nasal epithelia and its implication in rhinosinusitis. PLoS One. 2014;9(5):e98136. DOI: 10.1371/journal.pone.0098136. PMID: 24853033.

23. Park JA, Tschumperlin DJ. Chronic intermittent mechanical stress increases MUC5AC protein expression. Am J Respir Cell Mol Biol. 2009;41(4):459-66. DOI: 10.1165/rcmb.2008-0195OC. PMID: 19168703.

24. Deinhardt-Emmer S, Böttcher S, Häring C, Giebeler L, Henke A, Zell R, et al. SARS-CoV-2 causes severe epithelial inflammation and barrier dysfunction. J Virol. 2021;95(10):e00110-21. DOI: 10.1128/JVI.00110-21. PMID: 33692203.

25. Bilinska K, Jakubowska P, Von Bartheld CS, Butowt R. Expression of the SARS-CoV-2 entry proteins, ACE2 and TMPRSS2, in cells of the olfactory epithelium: identification of cell types and trends with age. ACS Chem Neurosci. 2020;11(11):1555-62. DOI: 10.1021/acschemneuro.0c00210. PMID: 32371031.

26. Pliss A, Kuzmin AN, Prasad PN, Mahajan SD. Mitochondrial dysfunction: a prelude to neuropathogenesis of SARS-CoV-2. ACS Chem Neurosci. 2022;13(3):308-12. DOI: 10.1021/acschemneuro.1c00675. PMID: 35041416.

27. Oliveira BR, Nehlmeier I, Kempf AM, Venugopalan V, Rehders M, Ceniza MEP, et al. Cytoskeletal β-tubulin and cysteine cathepsin L deregulation by SARS-CoV-2 spike protein interaction with the neuronal model cell line SH-SY5Y. Biochimie. 2024;226:49-61. DOI: 10.1016/j.biochi.2024.02.006. PMID: 38387807.

28. Aminpour M, Hameroff S, Tuszynski JA. How COVID-19 hijacks the cytoskeleton: therapeutic implications. Life (Basel). 2022;12(6):814. DOI: 10.3390/life12060814. PMID: 35743845.

29. Schreiner T, Allnoch L, Beythien G, Marek K, Becker K, Schaudien D, et al. SARS-CoV-2 infection dysregulates cilia and basal cell homeostasis in the respiratory epithelium of hamsters. Int J Mol Sci. 2022;23(9):5124. DOI: 10.3390/ijms23095124. PMID: 35563515.

30. Shi D, Komatsu K, Hirao M, Toyooka Y, Koyama H, Tissir F, et al. Celsr1 is required for the generation of polarity at multiple levels of the mouse oviduct. Development. 2014;141(23):4558-68. DOI: 10.1242/dev.115659. PMID: 25406397.

31. Boutin C, Labedan P, Dimidschstein J, Richard F, Cremer H, André P, et al. A dual role for planar cell polarity genes in ciliated cells. Proc Natl Acad Sci USA. 2014;111(30):E3129-38. DOI: 10.1073/pnas.1404988111. PMID: 25024228.

32. Dafinger C, Liebau MC, Elsayed SM, Hellenbroich Y, Boltshauser E, Korenke GC, et al. Mutations in KIF7 link Joubert syndrome with Sonic Hedgehog signaling and microtubule dynamics. J Clin Invest. 2011;121(7):2662-7. DOI: 10.1172/JCI43639. PMID: 21633168.

33. Rao VG, Subramanianbalachandar VA, Magaj MM, Redemann S, Kulkarni SS. Mechanisms of cilia regeneration in Xenopus multiciliated epithelium in vivo. EMBO Rep. 2025;26(8):2192-220. DOI: 10.1038/s44319-025-00414-8. PMID: 40087471.

34. Jang YJ, Myong NH, Park KH, Koo TW, Kim HG. Mucociliary transport and histologic characteristics of the mucosa of deviated nasal septum. Arch Otolaryngol Head Neck Surg. 2002;128(4):421-4. DOI: 10.1001/archotol.128.4.421. PMID: 11926916.

35. Pavlov SV, Avrunin OG, Zlepko SM, Bodyanskyi YeV. Intelligent Technologies in Medical Diagnosis, Treatment, and Rehabilitation: Monograph. Vinnytsia: PP TD "Edelweiss & K"; 2019. 260 p. [In Ukrainain].

36. Ismail HF, Abu E, Osman A, Omari A, Avrunin O, Bin S. The role of paranasal sinuses in the aerodynamics of the nasal cavities. Int J Life Sci Med Res. 2012;2(3):52-5. DOI: 10.5963/lsmr0203004.

Received: 15 Sep 2025
Accepted: 29 Dec 2025
Published: 31 Dec 2025

Cite in Vancouver style as: Bondarenko YaD, Shushliapina NO, Kalashnyk-Vakulenko YuM, Yashchenko MI. Pathophysiological mechanisms of mucociliary clearance function in patients with respiratory and olfactory disorders of functional-mechanical and viral origin. Inter Collegas. 2025;12(4):9p. In press. https://doi.org/10.35339/ic.2025.12.4.bsk